PAPER • OPEN ACCESS

Simple models for rope substructure mechanics: application to electro-mechanical lifts

To cite this article: I Herrera and S Kaczmarczyk 2016 *J. Phys.: Conf. Ser.* **721** 012008

View the article online for updates and enhancements.

Simple models for rope substructure mechanics: Application to electro-mechanical lifts

I Herrera[1a]**, S Kaczmarczyk**[2b]

[a]Escuela de Ingenierías Industriales, Universidad de Extremadura, Avda. de Elvas s/n, 06006 Badajoz, Spain

[b]School of Science and Technology, The University of Northampton, St. George's Avenue, Northampton, NN2 6JD, UK

[1]iherrera@unex.es, [2]stefan.kaczmarczyk@northampton.ac.uk

Abstract. Mechanical systems modelled as rigid mass elements connected by tensioned slender structural members such as ropes and cables represent quite common substructures used in lift engineering and hoisting applications. Special interest is devoted by engineers and researchers to the vibratory response of such systems for optimum performance and durability. This paper presents simplified models that can be employed to determine the natural frequencies of systems having substructures of two rigid masses constrained by tensioned rope/cable elements. The exact solution for free un-damped longitudinal displacement response is discussed in the context of simple two-degree-of-freedom models. The results are compared and the influence of characteristics parameters such as the ratio of the average mass of the two rigid masses with respect to the rope mass and the deviation ratio of the two rigid masses with respect to the average mass is analyzed. This analysis gives criteria for the application of such simplified models in complex elevator and hoisting system configurations.

1. Introduction

We focuses our attention on the mechanical substructure shown in figure 1 in which two lumped mass components M_1 and M_2 are connected by an elastic tensioned member/rope-piece of length l which can be the equivalent mechanical model of a number of common substructures in lift engineering and hoisting equipment. We are particularly interested in traction lift suspension ropes substructures. It should be mention that the system in figure 1 is a semi-definite system. Thus, there is a rigid body mode with zero frequency.

   The prediction of dynamic response of the suspension ropes is essential to understand and model the elevator system. In a typical lift installation the car/counterweight suspension system is formed by a number (n_R) of equally tensioned steel wire ropes acting in parallel, attached to the car frame at one end, passing over a traction sheave and diverter pulleys to the counterweight at the other end. The contact between the rope and traction sheave and diverter pulleys is specially critical, not only for the neccesity to produce the desired motion of the car but for its control, safety, and maintenance of relevant traction condition according to EN-81-20. If we assume that no slipping exists between the ropes and the traction sheave both sides of the rope can be represented by the simplified substructure shown in figure 1. Thus: M_1 would correspond to the traction sheave equivalent mass (rotary or linear)

for both sides and M_2 would correspond to the car mass for the frame side substructure or the counterweight mass for the counterweight side substructure. Another model from the opposite side to that free (M_1)-free (M_2) model shown in figure 1 is the fixed (M_1)-free (M_2) model which was extensively studied by Leung [2]. This model could be the best aproximation for static stopped elevator slings(brakes pressed) but its response wouldn't be affected at all by the lumped mass (M_1).
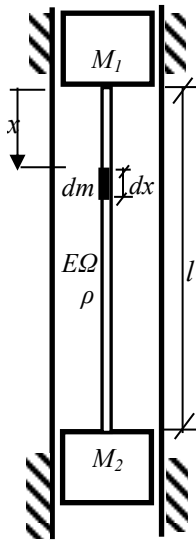

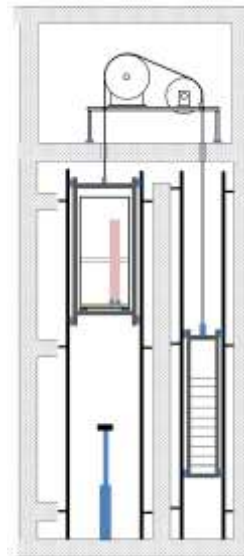**Figure 1.** Substructure of two rigid masses tensioned by a rope.

Figure 2. Elevator system schem.

The dynamic behavior of the mass suspension system can be analyzed by treating the ropes as linear distributed-parameter elastic members. To give criteria about the relative influence of the mechanical characteristics of the rope-pieces with respect to the joined up rigid masses properties and the method of analysis, several substructuring techniques were studied [2-3] and the system shown in figure 1 will be analyzed.

The dynamics of suspended ropes has been intensively studied. Several contributions from Zhu et al. [4-5] and Kaczmarczyk [6-7] give a wide and complete solution to the rope modelled as linear elastic continua. The assumptions for the car and counterweight as assemblies to be treated as rigid bodies are based on the low longitudinal elastic modulus of the rope whilst perfect flexural flexibility and high elastic modulus of the metallic components.

Typical analysis capable of generalization and modularity of complex systems is the application of the finite element method [8-9]. The continuous description of the rope is substituted by a finite number of sections/ elements, with their deformations described by equations in terms of unknowns displacements.

In the simplified models it is proposed to discretize the suspended rope- substructure using only one element. This has the advantage of maintaining small number of unknowns and equations and facilitates any further synthesizing strategy. In such an approach these models describe the elevator response well without significant loss of accuracy. Particularly, special interest is devoted to justify the application to suspended rope-substructures which were discretized to adopt a 6 degrees of freedom discrete model of the elevator system [1].

In a typical lift or elevator system the car and the counterweight are mounted in a frame/sling (see figure 2). Both are generally made of steel sections and fixed to each counter-part by bolts and nuts or by welding techniques [1]. Special attention is devoted to tighten the pieces to avoid noise during travel. Each of these components can be treated as an ideal rigid body constrained by the lift guiding system. In this arrangement the six degrees of freedom of a rigid body moving in space are reduced to only one (vertical translation) assuming ideal sliding joints between car-frame or counterweight and the guide rails.

2. Boundary-value problem solutions

Two rigid components of masses M_1 and M_2 are connected by an elastic tensioned rope-piece of length l (figure 1). The rope-piece is characterized by its density ρ, net cross-section area Ω and apparent elastic modulus E and then its total mass m ($m=\rho\Omega l$). Let us denote by M the average mass of M_1 and M_2. Then, two characteristics ratios of the system are intended to be analyzed: the ratio of the average rigid masses M with respect to the rope mass m, M/m and the ratio of the semi-difference mass $(M_1-M_2)/2$ with respect to the average mass, d:

$$d = \frac{\dfrac{M_1 - M_2}{2}}{M} \Rightarrow M_1 = M(1+d); M_2 = M(1-d) \tag{1}$$

The longitudinal vibrations (u) of the rope-piece are characterized by the differential equation [10]:

$$\ddot{u} - b^2 u'' = 0 \tag{2}$$

where the dot denotes the differentiation with respect to the time t and the prime denotes derivative with respect to x, and $b = \sqrt{E/\rho}$. The solution of (1) for stationary vibrations can be determined if u has the form $u = X(x) \cdot T(t)$ where X is a function of x only and T is a function of t only. Substituting this in (2) gives

$$b^2 \cdot X'' \cdot T = X \cdot \ddot{T} \tag{3}$$

By separating the variables,

$$T = A\cos(\omega t + \theta); X = C\sin\frac{\omega}{b}x + D\cos\frac{\omega}{b}x \tag{4}$$

where A, B and C are integration constants. Combining the constants yields:

$$u = \left(\bar{C}\sin\frac{\omega}{b}x + \bar{D}\cos\frac{\omega}{b}x\right)\cos(\omega t + \theta) \tag{5}$$

where $\bar{C} = AD$ and $\bar{D} = AD$.

The constants $\bar{C}$ and $\bar{D}$ are determined by the boundary conditions of the rope-piece and by the initial conditions of the vibration. The boundary conditions are:

$$\begin{aligned} &at\ x = 0:\ E\Omega \cdot u'(0,t) = M_1 \cdot \ddot{u}(0,t) \\ &at\ x = l:\ E\Omega \cdot u'(l,t) = -M_2 \cdot \ddot{u}(l,t) \end{aligned} \tag{6}$$

which leads to:

$$\begin{aligned} &E\Omega\frac{\omega}{b}\bar{C}\cdot\cos(\omega t + \theta) = M_1\omega^2\bar{D}\left[-\cos(\omega t + \theta)\right] \\ &E\Omega\frac{\omega}{b}\left(\bar{C}\cos\frac{\omega l}{b} - \bar{D}\sin\frac{\omega l}{b}\right)\cdot\cos(\omega t + \theta) = -M_2\omega^2\left(\bar{C}\sin\frac{\omega l}{b} + \bar{D}\cos\frac{\omega l}{b}\right)\left[-\cos(\omega t + \theta)\right] \end{aligned} \tag{7}$$

This set of equations is compatible and undetermined if:

$$tg\alpha = \frac{\alpha\left(\dfrac{M_1}{m} + \dfrac{M_2}{m}\right)}{\alpha^2 \dfrac{M_1}{m}\dfrac{M_2}{m} - 1} \tag{8}$$

where $\alpha = \omega l/b$. The solution of equation (8) gives n eigenvalues α_i $(i=1,...,n)$. Every α_i defines the frequency of the system ω_i in terms of the parameters M_1/m, M_2/m, l and b, so that the complete solution of (2) is of the form:

$$u = \sum_{i=1}^{i=\infty}\left(\overline{C}_i \, sin\frac{\omega_i}{b}x + \overline{D}_i \, cos\frac{\omega_i}{b}x\right)cos(\omega_i t + \theta_i) \tag{9}$$

Equation (8), which can be re-written in terms of parameters M and d as Equation (10), gives the eigenvale α_1 corresponding to the fundamental frequency ω_1 $(\omega_1 = \alpha_1 b/l)$.

$$tg\alpha = \frac{\alpha\left(\dfrac{2M}{m}\right)}{\alpha^2 \dfrac{(M - dM)}{m}\dfrac{(M + dM)}{m} - 1} = \frac{2\alpha\dfrac{M}{m}}{\alpha^2\left(\dfrac{M}{m}\right)^2(1 - d^2) - 1} \tag{10}$$

The eigenvalue α_1 which corresponds to the lowest root of (10) is listed for a number of mass M/m and d ratios in the table 1. It is evident that the first frequency of the substructure will be influenced by both the mass ratio and the deviation ratio. The limitation of this exact solution is the difficulty to be extended to damped and non steady state solutions. An alternative to the exact solution based on the frequency equation (10) capable of increasing complexity and modularity is that based on the finite element method (FEM).

Table 1. First frequency factor α_1 for a number of M/m and d ratios.

M/m	d=0	d=0.3	d=0.5
0.0100	3.0800	3.0800	3.0800
0.0200	3.0209	3.0209	3.0210
0.0300	2.9642	2.9643	2.9645
0.0400	2.9098	2.9101	2.9106
0.0500	2.8577	2.8582	2.8590
0.0600	2.8078	2.8085	2.8098
0.0700	2.7599	2.7610	2.7628
0.0800	2.7140	2.7154	2.7180
0.0900	2.6699	2.6718	2.6752
0.1000	2.6277	2.6301	2.6343
0.2000	2.2845	2.2933	2.3089
0.3000	2.0422	2.0575	2.0849
0.4000	1.8615	1.8820	1.9193
0.5000	1.7207	1.7451	1.7902
1.0000	1.3065	1.3391	1.4028
2.0000	0.9602	0.9931	1.0605
5.0000	0.6221	0.6482	0.7039
10.0000	0.4435	0.4635	0.5067

In the FEM approach the rope-piece is subdivided into a number of finite axially loaded bar elements of length l_e and linear interpolation for the spatial part $X(x)$ of the unknown displacement u is proposed which gives the oportunity to include the influence of damping, essential for modelling real elevator

systems. This drives to a finite consistent element with two degrees of freedom characterized dynamically [12] by the matrices $[m_e]$, $[k_e]$ and $[c_e]$ as follows:

$$[m]^e = m \begin{bmatrix} \dfrac{1}{3} & \dfrac{1}{6} \\ \dfrac{1}{6} & \dfrac{1}{3} \end{bmatrix}; [k]^e = \frac{E\Omega}{l^e} \begin{bmatrix} 1 & -1 \\ -1 & 1 \end{bmatrix}; [c]^e = \frac{c}{l^e} \begin{bmatrix} 1 & -1 \\ -1 & 1 \end{bmatrix} \qquad (11)$$

where c is the viscous damping coefficient in the rope that is assigned depending of the suspended overall mass and will be defined further on. If we discretize the rope-piece shown in Figure 1 by only one element following the Finite Element method, assemble together to the concentrated masses M_1 and M_2 and express the governing equations using the matrices of the system $[M]$, $[K]$ and $[C]$, force vector $[F]$ and unknown displacements $[u]$ we get:

$$[M][\ddot{u}] + [C][\dot{u}] + [K][u] = [F] \qquad (12)$$

where:

$$[M] = \begin{bmatrix} M_1 + \dfrac{m}{3} & \dfrac{m}{6} \\ \dfrac{m}{6} & M_2 + \dfrac{m}{3} \end{bmatrix}; [K] = \frac{E\Omega}{l} \begin{bmatrix} 1 & -1 \\ -1 & 1 \end{bmatrix}; [C] = \frac{c}{l} \begin{bmatrix} 1 & -1 \\ -1 & 1 \end{bmatrix} \qquad (13)$$

Another coarse simplified model for the dynamics shown in Figure 1 is based on the discrete approach in which the total mass of the rope is redistributed into two concentrated masses on its ends and these two masses are connected with and ideal equivalent spring/damper. Then we get the matrices as follows:

$$[M] = \begin{bmatrix} M_1 + \dfrac{m}{2} & 0 \\ 0 & M_2 + \dfrac{m}{2} \end{bmatrix}; [K] = \frac{E\Omega}{l} \begin{bmatrix} 1 & -1 \\ -1 & 1 \end{bmatrix}; [C] = \frac{c}{l} \begin{bmatrix} 1 & -1 \\ -1 & 1 \end{bmatrix} \qquad (14)$$

Finally, if we consider the rope massless, the matrices of the governing equations are:

$$[M] = \begin{bmatrix} M_1 & 0 \\ 0 & M_2 \end{bmatrix}; [K] = \frac{E\Omega}{l} \begin{bmatrix} 1 & -1 \\ -1 & 1 \end{bmatrix}; [C] = \frac{c}{l} \begin{bmatrix} 1 & -1 \\ -1 & 1 \end{bmatrix} \qquad (15)$$

We can compare these simplified models of the substructure shown in Figure 1 with the exact solution solving:

$$\left| -\omega^2[M] + [K] \right| = 0 \qquad (16)$$

which is the condition for getting the natural frequencies of the undamped system. The eigenvalue problem represented by Equation (16) can be easily solved using established numerical techniques

(implemented in software tools such as the '*eig*' MATLAB function). The analytical solution for the massless rope model gives the following fundamental frequency:

$$\omega_1 = \sqrt{\frac{2}{1-d^2}} \cdot \sqrt{\frac{E\Omega/l}{M}} \tag{17}$$
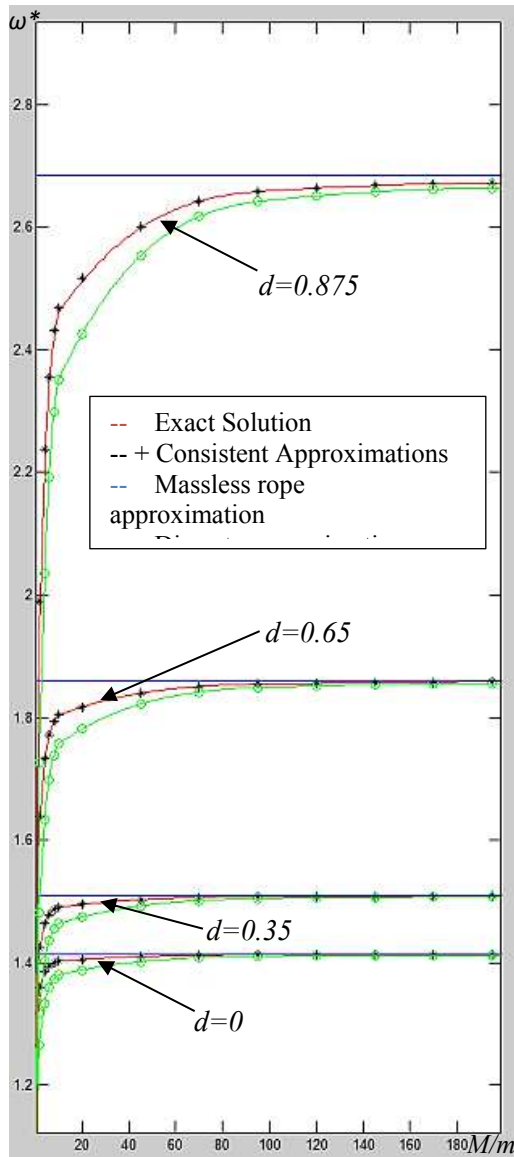
which is independent of the mass ratio *M/m*.

Figure 3. The first frequency dimensionless factor ω^* of the substructure shown in figure 1 against the mass ratio *M/m* for a number of deviation ratios *d* and models.

It can be shown that there is a simple closed-form formula for the models (14) and (15)

$$\omega_1 = \sqrt{\frac{k}{m_{eff}}} \tag{18}$$

where $k = E\Omega/l$ and $m_{eff} = \dfrac{m_1 m_2}{m_1 + m_2}$ where $m_i = M_i$, $i=1, 2$ for model (15) and $m_i = M_i + m/2$, $i=1, 2$ for model (14).

3. Results and Conclusions

Figure 3 shows the dimensionless parameter ω^* defined which is related to the first frequency of the substructure ω_1 ($\omega_1 = \alpha_1 b/l$), as a function of the mass ratio M/m for a number of deviation ratios.

$$\omega^* = \frac{\omega_1}{\sqrt{\dfrac{E\Omega/l}{M}}} = \frac{\omega_1}{\sqrt{\dfrac{E\Omega/l}{m}}}\sqrt{\frac{M}{m}} = \alpha_1\left(\frac{M}{m}, d\right)\sqrt{\frac{M}{m}} \tag{19}$$

It is observed how the consistent simplification gives the best approximation in practically every condition of mass and deviation ratios with respect to the other simplification models. Considering the rope massless -equations (15)- or using the discrete aproximation –equations (14)- gives a considerable error in the range of mass ratio which applies to elevator applications (*M/m=2* and *d=0*: α_1=0.9602 and ω^*=0.9602*(2)^0.5=1.3579 and by (19) ω^*_{aprox}= (2)^0.5, that is, an *3.98%* error), though it can be acceptable for coarse approximations.

We have studied the consistent approximation for a number of typical configurations of residential elevators (number of passengers n_P ranging from 4 to 16) in the car-frame sling which is worse case than that of the counterweight sling. We have considered both the rotary and the translational lift drive-car frame substructures (See table 2). The mass of the sling *m'* has been computed according to the number of ropes n_R and roping system (*n:1*). It is observed that the mass deviation *d* is always below 75.1% and the maximum mass ratio is above 1.46 (*M/m>1.46*) giving an error in the fundamental frequency in the range *0.3%-1.4%* after computing equation (10) and solving equation (16). The question that must be discussed now is whether the same results would arise by analyzing higher natural frequencies of the substructure.

Table 2. Application to car-frame sling of residential elevators

n_P	M_2 Car-frame (empty car) [kg]	M_1 Lift Drive +bedplate [kg]	M_1=0.75·I/R² Rotary lift drive [kg]	n_R(n:1)	ρ [kg/m]	m'=$\rho h n n_R$ (h=30m) [kg]	M [kg]	d	M/m'
4	167	245	400x72 : 53.97	3(1:1)	0.423	38.07	110	0.511	2.90
		203	240x110: 29.69	4(2:1)	0.179	42.96	98	0.698	2.29
6	167	310	400x87: 65.22	4(1:1)	0.423	50.76	116	0.438	2.29
		220	240x110 29.69	5(2:1)	0.179	53.7	98	0.698	1.83
8	167	300+50	400x102: 76.46	6(1:1)	0.423	76.14	122	0.372	1.60
		182+55	240x110 29.69	6(2:1)	0.179	64.4	98	0.698	1.53
13	241	350+75	400x72: 53.97	6(1:1)	0.423	76.14	148	0.634	1.94
		214+70	240x130 35.08	8(2:1)	0.179	85.92	138	0.746	1.61
16	247	450+100	400x102: 76.46	6(1:1)	0.610	109.8	161	0.527	1.47
		232+80	240x130: 35.08	9(2:1)	0.179	96.66	141	0.751	1.46

This was studied by Leung in the case of longitudinal vibrations in a fixed-free bar [2]. It is obvious that *p* natural frequencies can only be predicted by a *p* degree-of-freedom mathematical model. It is evident that the accuracy of the predicted frequencies decreases with the increase of the number of degrees of freedom.

The consistent simplification is the best one element-substructure. The application of simple models to suspended rope-substructures of only 6 degrees of freedom discrete model of an elevator system seems to be adequate and coherent. In future work, the effect of increasing the number of

elements of the rope-piece using the FEM method for increasing knowledge in the dynamic response of the elevator system, specially to higher frequencies and retardation estimations, must be analyzed.

References
[1]   Sicilia J R, Alonso F J and Herrera I 2015 Mechanical Discrete Simulator of the Electro-mechanical Lift with n:1 roping *The 5th Symposium on Mechanics of Slender Structures (MoSS2015)* 21-22 September 2015 Northampton, UK.
[2]   Leung A Y T 1993 *Dynamic Stiffness and Substructures* Springer-Verlag London
[3]   Craig RR 1995 Substructure Methods in Vibration *Transactions of the ASME* **117**
[4]   WD Zhu, H Ren An Accurate Spatial Discretization and Substructure Method With Application to Moving Elevator Cable-Car Systems—Part I: Methodology *Journal of Vibration and Acoustics* october 2013 **135**
[5]   Zhu WD and Ren H 2013 An Accurate Spatial Discretization and Substructure Method With Application to Moving Elevator Cable-Car Systems—Part II: Application. *Journal of Vibration and Acoustics* october 2013 **135**
[6]   Kaczmarczyk S and Mirhadizadeh S 2014 Modelling, Simulation and Experimental Validation of Nonlinear Dynamic Interactions in an Aramid Rope System *Applied Mechanics and Materials Special Issue: Dynamics and Control of Technical Systems* **706** 117-127 1662-7482
[7]   Kaczmarczyk S and Picton P D 2013 The Prediction of Nonlinear Responses and Active Stiffness Control of Moving Slender Continua Subjected to Dynamic Loadings in Vertical Host Structures *The International Journal of Acoustics and Vibration* **18**(1) 39–44
[8]   Stokey W F 2002 Vibration of systems having distributed mass and elasticity *Shock and Vibration Handbook* Chapter 7. Fifth Edition. Cyril M. Harris. Mc Graw Hill.
[9]   Alarcón E 1990 Cálculo Dinámico Chapter 4 *Cálculo Matricial de Estructuras* Editorial Reverté.
[10]   Belluzi O 1971 *Ciencia de la Construcción IV*. 443-445 Editorial Aguilar